AD-A088 287 WASHINGTON UNIV SEATTLE DEPT OF MECHANICAL ENGINEERING F/G 20/11
DYNAMIC MIXED MODE FRACTURE.(U)
AUG 80 A S KOBAYASHI, M RAMULU N00014-76-C-0060
UNCLASSIFIED TR-39 NL

1 OF 1
AD A088287

END
DATE FILMED
9-80
DTIC

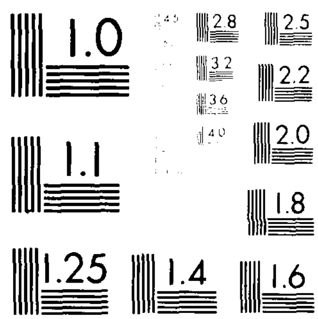

MICROCOPY RESOLUTION TEST CHART

Office of Naval Research

Contract N00014-76-0060 NR 064-478

Technical Report No. 39

DYNAMIC MIXED MODE FRACTURE

by

A. S. Kobayashi and M. Ramulu

August 1980

The research reported in this technical report was made possible through support extended to the Department of Mechanical Engineering, University of Washington, by the Office of Naval Research under Contract N00014-76-C-0060 NR 064-478. Reproduction in whole or in part is permitted for any purpose of the United States Government.

Department of Mechanical Engineering
College of Engineering
University of Washington

DYNAMIC MIXED MODE FRACTURE

A. S. Kobayashi and M. Ramulu

Department of Mechanical Engineering, University of Washington

ABSTRACT

A newly developed data reduction process was used to reevaluate dynamic photoelastic results and to extract dynamic stress intensity factors, K_I^{dyn} and K_{II}^{dyn}, associated with curved and branched cracks in fracturing Homalite - 100 plates. A branching stress intensity factor approximately 5 times the fracture toughness was identified for this material. Moderate to severe crack curvings were associated with a K_I^{dyn} and K_{II}^{dyn} ratio as low as 0.05, but with positive remote stress component, σ_{ox}.

INTRODUCTION

Two dimensional dynamic photoelasticity has been used by Dally and his associates [1,2] and by the author and his associates [3,4] to determine experimentally the dynamic stress intensity factor K_I^{dyn}, surrounding a propagating crack and to establish a dynamic fracture toughness, K_{ID}, versus crack velocity $\dot{a}$, relation which may control dynamic fracture. This use of dynamic photoelasticity in studying dynamic fracture has been eloquently described by J. W. Dally in his recent article [1]. As noted by Dally, the data reduction procedure used by most investigators in the past for calculating K_I^{dyn}, from the transient isochromatics surrounding the propagating crack tip, was restricted to Mode I crack tip deformation. A theoretical, near-field, static isochromatics was first equated to the recorded experimental dynamic isochromatics and the resultant static stress intensity factor of the former was considered the dynamic stress intensity factor of the latter [2,5]. Error estimates for using a near-field stress to extract the Mode I dynamic stress intensity factor have been made by several investigators [6-8] and in particular, exhaustively by Rossmanith and Irwin [8].

Studies of the static isochromatic patterns under mixed mode loading conditions, i.e. in the presence of combined K_I and K_{II} crack tip deformations were made by C. W. Smith [9,10], Gdousto and Theocaris [11] and more recently by Dally and Sanford [12,13] and Rossmanith [14]. These mixed mode isochromatics are all characterized by their unsymmetric patterns with respect to the straight crack line. It is also interesting to note that the shapes of these static isochromatics are strongly influenced by the higher order terms, i.e. terms other than K_I and K_{II}. In particular, the second order term of σ_{ox}, commonly referred to as the remote stress component, will distort the symmetry of the isochromatics by significant stretching and shortening of the upper and lower loop system [14]. For a pure mode II crack tip deformation, the isochromatic loop straddles the crack tip as shows in Figure 1 where a nearly pure shear state of stress is generated around branched cracks. The mode II stress intensity factors K_{II}, and remote stress components σ_{ox}, associated with these isochromatics are listed in the following Table 1.

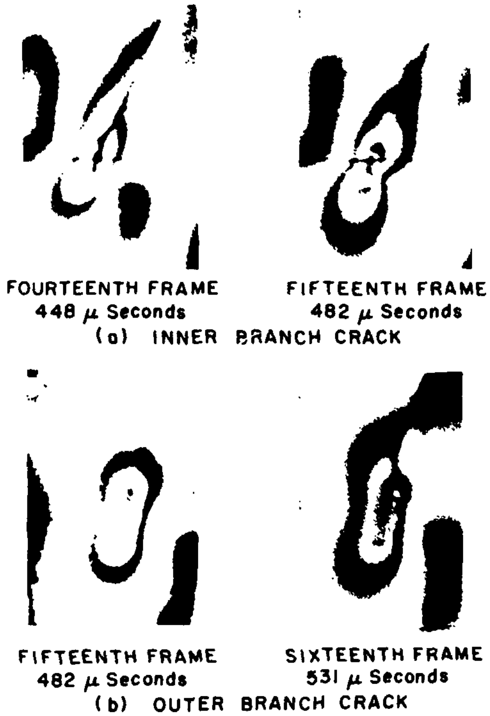

Fig. 1 Typical Mode II Dynamic Isochromatic Patterns of Arresting Branched Cracks. Homalite-100 Single Edge Notched Specimen Under Fixed-Grip Loading. Specimen No. B5

Table 1. K_{II} and σ_{ox} for Arrested Branch Cracks in Fig. 1

(a) Inner Branch Crack

	14th Frame	15th frame
K_{II}	0.4 MPa√m	0.44 MPa√m
σ_{ox}	0.32 MPa	-0.04 MPa

(b) Outer Branch Crack

	15th frame	16th frame
K_{II}	0.44 MPa√m	0.41 MPa√m
σ_{ox}	0.18 MPa	0.08 MPa

In actual dynamic photoelastic analysis of dynamic fracture, dynamic isochromatics surrounding a running crack often exhibits moderate unsymmetry but such photoelastic patterns were heretofore considered experimental abnormalities and were ignored by averaging the unsymmetric patterns during the data reduction process. Careful postmortem inspection of the fracture specimens, however, show that the slightly unsymmetric isochromatics are often associated with slightly curved crack paths which undoubtedly are caused by the small dynamic K_{II}^{dyn}, coexisting with the dominating dynamic K_I^{dyn} value. This effect is akin to the small but noticeable influence of a small K_{II} on fatigue crack propagation reported fifteen years ago [15]. The exact relation between the amount of crack curving and the dynamic K_I and possibly other higher order terms of the near field stresses associated with the propagating crack tip would thus provide a dynamic crack propagation law under mixed-mode crack tip deformation similar to the K_{ID} versus $\dot{a}$ relation under consideration for Mode I dynamic crack propagation.

With the development of a data reduction procedure for evaluating K_{II} together with K_I^{dyn} values, it became possible to investigate experimentally the role of mixed mode dynamic near field stresses in dynamic fracture. The authors used such procedure to evaluate the stress intensity factors associated with crack branching and crack curving [16]. The purpose of this paper is to use this data reduction procedure to further extract K_I^{dyn} and K_{II}^{dyn} from the previously recorded dynamic isochromatics surrounding running crack tips of curved and branched cracks.

DATA REDUCTION PROCEDURE

A three parameter, mixed mode, near-field state of stresses surrounding a crack propagating at constant velocity [17,18] was used to derive a relation between the Modes I and II dynamic stress intensity factors, K_I^{dyn} and K_{II}^{dyn}, and the remote stress component σ_{ox}, and the dynamic isochromatics. This relation together with an overdeterministic, least-square method formed the basis of a data reduction procedure for extracting the three dynamic parameters K_I^{dyn} and K_{II}^{dyn} and σ_{ox} from the recorded dynamic photoelastic pattern surrounding a running crack. Further details of this data reduction procedure can be found in Reference [16].

Figure 2 shows two frames out of a 16-frame dynamic photoelastic record of a curving crack in a notch bend specimen 9.58mm (3/8 inch) thick, 88.9 x 400mm (3 1/2 x 15 3/4 inch) Homalite-100 beam with a blunt initial crack of 6.4mm (7/32 inch) in length and which was impact loaded by a drop weight of 1.48 kg (3.25 lbs) [19]. The crack emanated from the blunt saw-cut pre-crack and propagated through much of the height of the beam prior to curving as it approached the region of impact loading. Further details of the experimental setup, crack velocity measurements and dynamic calibration of the Homalite-100 material used are found in Reference [19]. Figure 3 shows the K_I^{dyn} and K_{II}^{dyn} and σ_{ox} variations obtained from the dynamic photoelastic patterns preceding and immediately after the crack curving shown in Figure 2. The negligible K_{II}^{dyn} with respect to the K_I^{dyn} leads to speculation that the important factor governing the crack curving is not the K_{II} component of the mixed mode local dynamic state of stress, but rather the σ_{ox} component which heretofore was ignored in past static analyses. The directional stability of the static Mode I crack extension with σ_{ox} as a dominant factor, however, has been presented recently [20] and thus it is conceivable that the second order term, i.e. σ_{ox} in the dynamic near-field stresses, may also govern the crack path of a rapidly propagating crack. Crack curving associated with the large positive σ_{ox} values in Fig. 3 tends to confirm this speculation.

Fig. 2 Typical Dynamic Isochromatics of a Curved Crack. Homalite-100 notch bend specimen. Specimen No. 1-C042574

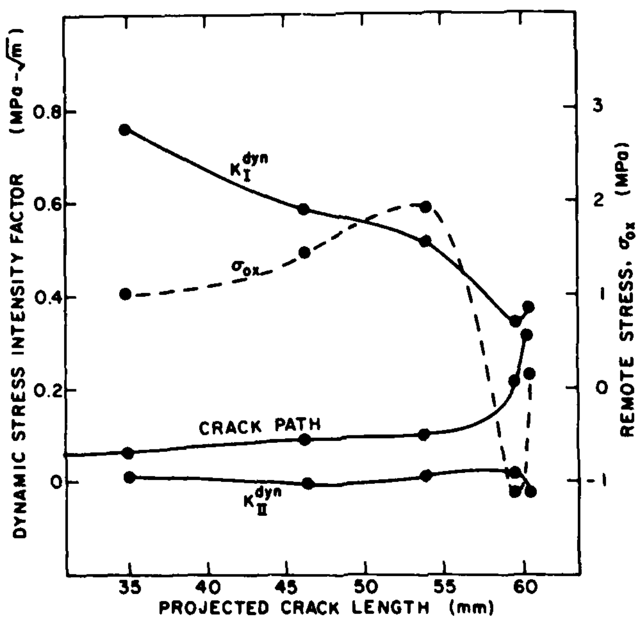

Fig. 3 Modes I and II Dynamic Stress Intensity Factors of the Curved Crack Shown in Fig. 2.

Figure 4 shows a slightly slanted crack and the associated K_I^{dyn}, K_{II}^{dyn} and σ_{ox} in a fracturing, wedge-loaded, double cantilever beam specimen of 9.6mm (3/8 inch) thick, 76.2 x 152.4mm (3 x 6 inch) Homalite-100 plate. Details of this experimental setup, etc., can be found in Reference [21]. Some fluctuations in K_I^{dyn} and K_{II}^{dyn} throughout the crack propagation history is noted. Again, the consistently low K_{II}^{dyn} values and the large positive σ_{ox} associated with significant crack curving tend to verify the previous finding regarding the importance of σ_{ox} in dynamic crack curving. It appears then that a fracture dynamic theory comparable to that of Ref. [20] and in the presence of small but non-negligible K_{II}^{dyn} may provide insight to dynamic crack curving.

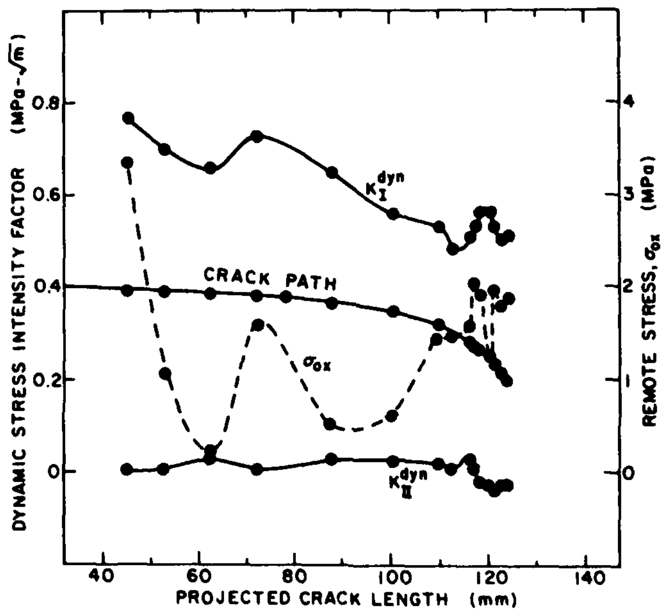

Fig. 4 Modes I and II Dynamic Stress Intensity Factors of a Slanted Crack in a Wedge-Loaded Rectangular Double Cantilever Specimen. Homalite-100 Specimen No. L31S-030274.

Figure 5 shows two dynamic photoelastic patterns of a branched crack in a single edge-notched 9.5mm (3/8 inch) thick, 254 x 254mm (10 x 10 inch) Homalite-100 plate subjected to fixed grip loading condition. Other branched cracks from this same specimen were shown in Fig. 1 and the experimental details of this test can be found in Reference [2]. As shown in Fig. 5, within the 49 micro-second interval, the propagating crack turned about 74° and arrested. The mixed Mode stress intensity factors prior to this severe crack kinking were K_I^{dyn} = 0, K_{II}^{dyn} = 0.41 MPa$\sqrt{m}$ and σ_{ox} = 0.18 MPa. After crack kinking at which time the crack arrested, K_I = 0.34 MPa$\sqrt{m}$, K_{II} = 0.08 MPa$\sqrt{m}$ and σ_{ox} = 1.4 MPa. This severe crack curving, i.e. crack kinking can also occur under the more traditional high K_{II} state of stress.

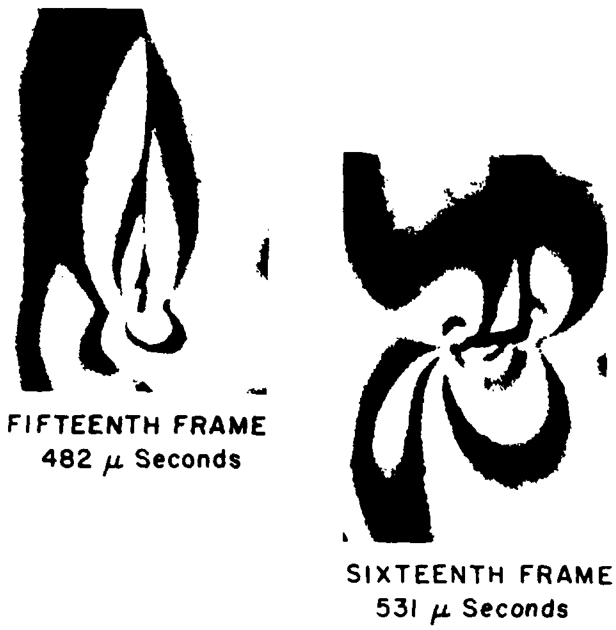

Fig. 5 Dynamic Isochromatics Prior To and After Crack Kinking. Homalite-100 Single Edge Notched Specimen Under Fixed Grip Loading. Specimen No.B5

The above three sets of data are obviously not sufficient to establish a dynamic crack curving criterion. Quantitative correlation of K_I^{dyn}, K_{II}^{dyn} and σ_{ox} with the degree of crack curving as well as the possible dependence on crack velocity are lacking at this time.

CRACK BRANCHING

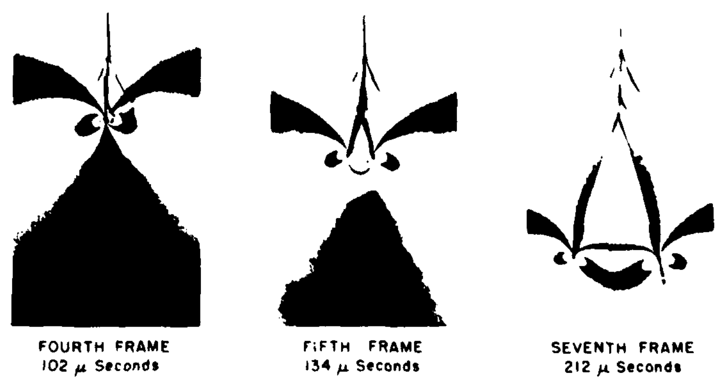

Fig. 6 Typical Crack Branching Dynamic Photoelastic Patterns Homalite-100 Single Edge Notched Specimen (Fixed Grip Loading) Specimen No. B8.

Figure 6 shows three frames out of a 16-frame dynamic photoelastic record of a crack propagating and branching in a 3.2mm (1/8 inch) thick, 254 x 254mm (10 x 10 inch) Homalite-100 plate loaded under fixed grip tension. Details of the experiment can be found in Reference [22].

Figure 7 shows the K_I^{dyn} and K_{II}^{dyn} for two branches of the cracks shown in Figure 6. By extrapolating the K_I^{dyn} associated with two branch cracks, an after-branching K_I^{dyn} = 1.2 MPa $\sqrt{m}$ (10.90 psi$\sqrt{in.}$) and K_{II}^{dyn} = 0.45 MPa $\sqrt{m}$ (410 psi $\sqrt{in}$) are obtained. The branching stress intensity factor, i.e. immediately prior to branching, is estimated to be K_I^{dyn} = 2.03 MPa $\sqrt{m}$ (1850 psi $\sqrt{in}$).

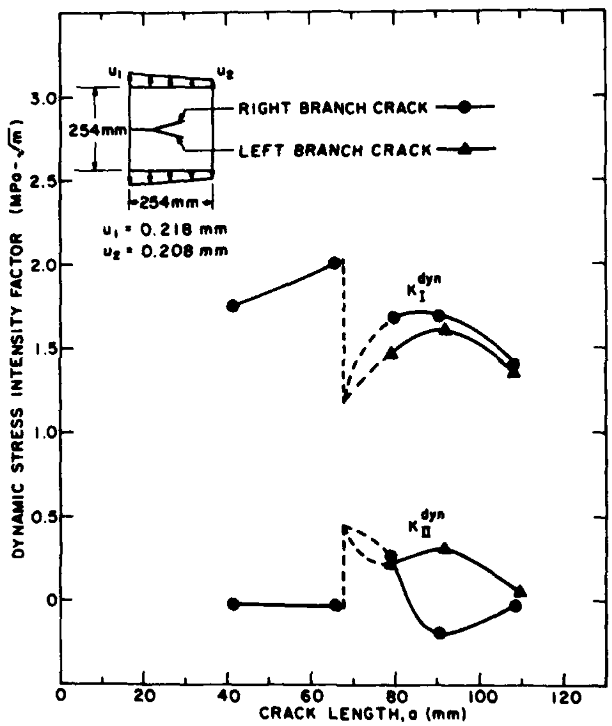

Fig. 7 Modes I and II Dynamic Stress Intensity Factors of the Branched Cracks Shown in Fig. 6.

Figure 8 shows another set of K_I^{dyn} and K_{II}^{dyn} for two branch cracks in a similar dynamic photoelastic experiment [20]. By extrapolating the K_I^{dyn} associated with the only readable right branch data, an after branching K_I^{dyn} = 1.02 MPa $\sqrt{m}$ (920 psi $\sqrt{in}$) and K_{II}^{dyn} = -0.2 MPa $\sqrt{m}$ (180 psi $\sqrt{in}$) are obtained. The extrapolated dynamic stress intensity factors prior to branching are K_I^{dyn} = 2.03 MPa $\sqrt{m}$ (1850 psi $\sqrt{in}$) and $K_{II}^{dyn} \doteq 0$.

The average branching and after-branching stress intensity factors of the above two experiments as well as those for the single experiment reported in Reference [15] yield the following:

Branching $K_I^{dyn} = 2.03$ MPa $\sqrt{m}$ (1850 psi $\sqrt{in}$)

$K_{II}^{dyn} \doteq 0$

After Branching $K_I^{dyn} = 1.0$ MPa $\sqrt{m}$ (950 psi $\sqrt{in}$)

$K_{II}^{dyn} = 0.2$ MPa $\sqrt{m}$ (180 psi $\sqrt{in}$)

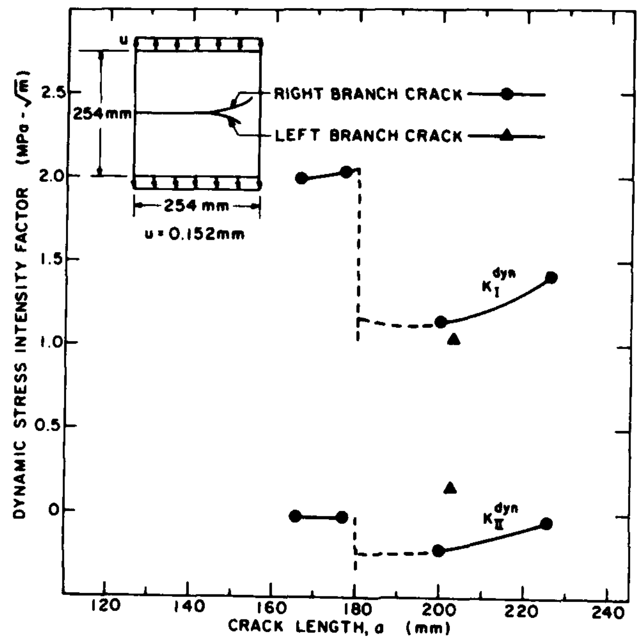

Fig. 8 Model I and II Dynamic Stress Intensity Factors of a Branched Crack in a Homalite-100 Single Edge Notched Specimen Under Fixed Grip Loading. Specimen No. B9.

The above branching K_I^{dyn} data is identical to that quoted in Reference [1]. The ratio of before over after K_I^{dyn} of 2.03/1.0 ≑ 2.0 is consistent with the postulate that crack branching occurs to dissipate fracture energy along two propagating cracks but is higher than the expected $\sqrt{2}$ value. It is also interesting to note that K_{II}^{dyn} which is prior to crack branching regains a small magnitude immediately after crack branching and is consistent with the static results of Reference [23].

DISCUSSIONS

The above dynamic photoelastic data on crack curving and crack branching should be considered as preliminary since the data is not sufficient in quantity for establishing a dynamic crack curving or a crack branching criteria. Evaluation of the accumulated dynamic photoelastic experiments using the newly developed data reduction procedure is continuing and the new crack curving and crack branching dynamic photoelastic experiments are planned.

ACKNOWLEDGEMENT

The results of this investigation were obtained in a research contract funded by the Office of Naval Research under Contract N00014-76-C-0060 NR 064-478. The authors wish to acknowledge the support and encouragement of Dr. N. R. Perrone of ONR during the course of this investigation.

REFERENCES

[1] Dally, J. W., "Dynamic Photoelastic Studies of Fracture", Experimental Mechanics, Vol. 19, No. 10, October 1979, pp. 349-367.

[2] Kobayashi, T. and Dally, J. W., "The Relation Between Crack Velocity and Stress Intensity Factor in Birefringent Polymers", Fast Fracture and Crack Arrest, (edited by G. T. Hahn and M. F. Kanninen), ASTM STP 627m 1977, pp. 257-273.

[3] Bradley, W. B. and Kobayashi, A. S., "An Investigation of Propagating Crack by Dynamic Photoelasticity", Experimental Mechanics, Vol. 10, No. 3, 1970, pp. 103-113.

[4] Bradley, W. B. and Kobayashi, A. S., "Fracture Mechanics - A Photoelastic Investigation", Engineering Fracture Mechanics, Vol. 3, 1971, pp. 317-332.

[5] Irwin, G. R., "Discussion of the Dynamic Stress Distribution Surrounding A Running Crack - A Photoelastic Analysis", Proc. of SESA, Vol. 16, No. 1, 1958, pp. 93-96.

[6] Kobayashi, A. S., Wade, B. G. and Bradley, W. B., "Fracture Dynamics of Homalite-100", Deformation and Fracture of High Polymers, (edited by H. H. Kausch, J. A. Hassell and R. I. Jafee), Plenum Press, New York, 1973, pp. 487-500.

[7] Irwin, G. R., Dally, J. W., Kobayashi, T., Fourney, W. L., Etheridge, M. J., and Rossmanith, H. P., "On the Determination of the $\dot{a}$-K relationships for Birefringent Polymers", Experimental Mechanics, Vol. 19, No. 4, 1979, pp. 121-128.

[8] Rossmanith, H. P. and Irwin, G. R., "Analysis of Dynamic Isochromatic Crack-Tip Stress Patterns", University of Maryland Report, 1979.

[9] Smith, D. G. and Smith, C. W., "Photoelastic Determination of Mixed Mode Stress Intensity Factors", Engineering Fracture Mechanics, Vol. 4, No. 2, 1972, pp. 357-366.

[10] Smith, C. W., Jolles, M. and Peters, W. H., "Stress Intensities for Crack Emanating from Pin-Loaded Holes", Flaw Growth and Fracture, ASTM STP 631, 1977, pp. 190-201.

[11] Gdoutos, E. E., and Theocaris, P. S., A Photoelastic Determination of Mixed-Mode Stress Intensity Factors", Experimental Mechanics, Vol. 18, March 1978, pp. 87-96.

[12] Dally, J. W. and Sanford, R. J., "Classification of Stress-Intensity Factors from Isochromatic Fringe Patterns", Experimental Mechanics, Vol. 18, No. 12, Dec. 1978, pp. 441-448.

[13] Sanford, R. J. and Dally, J. W., "A General Method for Determining Mixed-Mode Stress Intensity Factors from Isochromatic Fringe Patterns", Engineering Fracture Mechanics, Vol. 11, 1979, pp. 621-633.

[14] Rossmanith, H. P., "Analysis of Mixed-Mode Isochromatic Crack-Tip Fringe Patterns", Acta Mechanics, Vol. 34, 1979, pp. 1-38.

[15] Iida, S. and Kobayashi, A. S., "Crack Propagation Rate in 7075-T6 Plates Under Cyclic Tensile and Transverse Shear Loading", J. of Basic Engineering, Trans. of ASME, Vol. 91, Series D (4), Dec. 1964, pp. 764-769.

[16] Kobayashi, A. S. and Ramulu, M., "Dynamic Stress Intensity Factors for Unsymmetric Dynamic Isochromatics", to be published in Experimental Mechanics.

[17] Freund, L. B., "Dynamic Crack Propagation", The Mechanics of Fracture, Vol. 19, edited by F. Erdogan, ASME, 1976, pp. 105-134.

[18] Freund, L. B., "The Mechanics of Dynamic Shear Crack Propagation", Journal of Geophysical Research, Vol. 84, No. 35, 1978, pp. 2199-2209.

[19] Kobayashi, A. S. and Chan, C. F., "A Dynamic Photoelastic Analysis of Dynamic-tear-test Specimen", Experimental Mechanics, Vol. 16, No. 5, May 1976, pp. 176-181.

[20] Streit, R. amd Finnie, I, "An Experimental Investigation of Crack-path Directional Stability", Experimental Mechanics, Vol. 20, No. 1, January 1980, pp. 17-23.

[21] Kobayashi, A. S., Mall, S. amd Lee, M. H., "Fracture Dynamics of Wedge-Loaded Double Cantilever Beam Specimen", Cracks and Fracture, ASTM STP, 601, June 1976, pp. 274-290.

[22] Kobayashi, A. S., Wade, B. G., Bradley, W. B. and Chiu, S. T., "Crack Branching in Homalite-100 Sheets", Engineering Fracture Mechanics, Vol. 6, 1974, pp. 81-92.

[23] Kalthoff, J. F., "On the Propagation Direction of Bifurcated Cracks", Dynamic Crack Propagation (edited by G. C. Sih), Noordhoff International Leyden, 1973, pp. 449-458.

Part 1 - Government
Administrative and Liaison Activities

Office of Naval Research
Department of the Navy
Arlington, Virginia 22217
Attn: Code 474 (2)
Code 471
Code 200

Director
Office of Naval Research
Branch Office
666 Summer Street
Boston, Massachusetts 02210

Director
Office of Naval Research
Branch Office
536 South Clark Street
Chicago, Illinois 60605

Director
Office of Naval Research
New York Area Office
715 Broadway - 5th Floor
New York, New York 10003

Director
Office of Naval Research
Branch Office
1030 East Green Street
Pasadena, California 91106

Naval Research Laboratory (6)
Code 2627
Washington, D.C. 20375

Defense Documentation Center (12)
Cameron Station
Alexandria, Virginia 22314

Navy

Undersea Explosion Research Division
Naval Ship Research and Development Center
Norfolk Naval Shipyard
Portsmouth, Virginia 23709
Attn: Dr. E. Palmer, Code 177

Navy (Con't.)

Naval Research Laboratory
Washington, D.C. 20375
Attn: Code 8400
8410
8430
8440
6300
6390
6380

David W. Taylor Naval Ship Research and Development Center
Annapolis, Maryland 21402
Attn: Code 2740
28
281

Naval Weapons Center
China Lake, California 93555
Attn: Code 4062
4520

Commanding Officer
Naval Civil Engineering Laboratory
Code L31
Port Hueneme, California 93041

Naval Surface Weapons Center
White Oak
Silver Spring, Maryland 20910
Attn: Code R-10
G-402
K-82

Technical Director
Naval Ocean Systems Center
San Diego, California 92152

Supervisor of Shipbuilding
U.S. Navy
Newport News, Virginia 23607

Navy Underwater Sound Reference Division
Naval Research Laboratory
P.O. Box 8337
Orlando, Florida 32806

Navy (Con't.)

Chief of Naval Operations
Department of the Navy
Washington, D.C. 20350
Attn: Code OP-098

Strategic Systems Project Office
Department of the Navy
Washington, D.C. 20376
Attn: NSP-200

Naval Air Systems Command
Department of the Navy
Washington, D.C. 20361
Attn: Code 5302 (Aerospace and Structures)
604 (Technical Library)
320B (Structures)

Naval Air Development Center
Warminster, Pennsylvania 18974
Attn: Aerospace Mechanics
Code 606

U.S. Naval Academy
Engineering Department
Annapolis, Maryland 21402

Naval Facilities Engineering Command
200 Stovall Street
Alexandria, Virginia 22332
Attn: Code 03 (Research and Development)
04B
045
14114 (Technical Library)

Naval Sea Systems Command
Department of the Navy
Washington, D.C. 20362
Attn: Code 05R
312
322
323
05R
32R

Navy (Con't.)

Commander and Director
David W. Taylor Naval Ship Research and Development Center
Bethesda, Maryland 20084
Attn: Code 042
17
172
173
174
1800
1844
012.2
1900
1901
1945
1960
1962

Naval Underwater Systems Center
Newport, Rhode Island 02840
Attn: Dr. R. Trainor

Naval Surface Weapons Center
Dahlgren Laboratory
Dahlgren, Virginia 22448
Attn: Code G04
G20

Technical Director
Mare Island Naval Shipyard
Vallejo, California 94592

U.S. Naval Postgraduate School Library
Code 0384
Monterey, California 93940

Webb Institute of Naval Architecture
Attn: Librarian
Crescent Beach Road, Glen Cove
Long Island, New York 11542

Army

Commanding Officer (2)
U.S. Army Research Office
P.O. Box 12211
Research Triangle Park, NC 27709
Attn: Mr. J. J. Murray, CRD-AA-IP

Army (Con't.)

Watervliet Arsenal
MAGGS Research Center
Watervliet, New York 12189
Attn: Director of Research

U.S. Army Materials and Mechanics Research Center
Watertown, Massachusetts 02172
Attn: Dr. R. Shea, DRXMR-T

U.S. Army Missile Research and Development Center
Redstone Scientific Information Center
Chief, Document Section
Redstone Arsenal, Alabama 35809

Army Research and Development Center
Fort Belvoir, Virginia 22060

NASA

National Aeronautics and Space Administration
Structures Research Division
Langley Research Center
Langley Station
Hampton, Virginia 23365

National Aeronautics and Space Administration
Associate Administrator for Advanced Research and Technology
Washington, D.C. 20546

Air Force

Wright-Patterson Air Force Base
Dayton, Ohio 45433
Attn: AFFDL (FB)
(FBR)
(FBE)
(FBS)
AFML (MBM)

Air Force (Con't.)

Chief Applied Mechanics Group
U.S. Air Force Institute of Technology
Wright-Patterson Air Force Base
Dayton, Ohio 45433

Chief, Civil Engineering Branch
WLRC, Research Division
Air Force Weapons Laboratory
Kirtland Air Force Base
Albuquerque, New Mexico 87117

Air Force Office of Scientific Research
Bolling Air Force Base
Washington, D.C. 20332
Attn: Mechanics Division

Department of the Air Force
Air University Library
Maxwell Air Force Base
Montgomery, Alabama 36112

Other Government Activities

Commandant
Chief, Testing and Development Division
U.S. Coast Guard
1300 E Street, NW.
Washington, D.C. 20226

Technical Director
Marine Corps Development and Education Command
Quantico, Virginia 22134

Director Defense Research and Engineering
Technical Library
Room 3C128
The Pentagon
Washington, D.C. 20301

Other Government Activities (Con't)

Dr. M. Gaus
National Science Foundation
Environmental Research Division
Washington, D.C. 20550

Library of Congress
Science and Technology Division
Washington, D.C. 20540

Director
Defense Nuclear Agency
Washington, D.C. 20305
Attn: SPSS

Mr. Jerome Persh
Staff Specialist for Materials and Structures
OUSDR&E, The Pentagon
Room 3D1089
Washington, D.C. 20301

Chief, Airframe and Equipment Branch
FS-120
Office of Flight Standards
Federal Aviation Agency
Washington, D.C. 20553

National Academy of Sciences
National Research Council
Ship Hull Research Committee
2101 Constitution Avenue
Washington, D.C. 20418
Attn: Mr. A. R. Lytle

National Science Foundation
Engineering Mechanics Section
Division of Engineering
Washington, D.C. 20550

Picatinny Arsenal
Plastics Technical Evaluation Center
Attn: Technical Information Section
Dover, New Jersey 07801

Maritime Administration
Office of Maritime Technology
14th and Constitution Avenue, NW.
Washington, D.C. 20230

PART 2 - Contractors and Other Technical Collaborators

Universities

Dr. J. Tinsley Oden
University of Texas at Austin
345 Engineering Science Building
Austin, Texas 78712

Professor Julius Miklowitz
California Institute of Technology
Division of Engineering and Applied Sciences
Pasadena, California 91109

Dr. Harold Liebowitz, Dean
School of Engineering and Applied Science
George Washington University
Washington, D.C. 20052

Professor Eli Sternberg
California Institute of Technology
Division of Engineering and Applied Sciences
Pasadena, California 91109

Professor Paul M. Naghdi
University of California
Department of Mechanical Engineering
Berkeley, California 94720

Professor A. J. Durelli
Oakland University
School of Engineering
Rochester, Missouri 48063

Professor F. L. DiMaggio
Columbia University
Department of Civil Engineering
New York, New York 10027

Professor Norman Jones
The University of Liverpool
Department of Mechanical Engineering
P. O. Box 147
Brownlow Hill
Liverpool L69 3BX
England

Professor E. J. Skudrzyk
Pennsylvania State University
Applied Research Laboratory
Department of Physics
State College, Pennsylvania 16801

Universities (Con't.)

Professor J. Klosner
Polytechnic Institute of New York
Department of Mechanical and
Aerospace Engineering
333 Jay Street
Brooklyn, New York 11201

Professor R. A. Schapery
Texas A&M University
Department of Civil Engineering
College Station, Texas 77843

Professor Walter D. Pilkey
University of Virginia
Research Laboratories for the
Engineering Sciences and
Applied Sciences
Charlottesville, Virginia 22901

Professor K. D. Willmert
Clarkson College of Technology
Department of Mechanical Engineering
Potsdam, New York 13676

Dr. Walter E. Haisler
Texas A&M University
Aerospace Engineering Department
College Station, Texas 77843

Dr. Hussein A. Kamel
University of Arizona
Department of Aerospace and
Mechanical Engineering
Tucson, Arizona 85721

Dr. S. J. Fenves
Carnegie-Mellon University
Department of Civil Engineering
Schenley Park
Pittsburgh, Pennsylvania 15213

Dr. Ronald L. Huston
Department of Engineering Analysis
University of Cincinnati
Cincinnati, Ohio 45221

Universities (Con't)

Professor G. C. M. Sih
Lehigh University
Institute of Fracture and
Solid Mechanics
Bethlehem, Pennsylvania 18015

Professor Albert S. Kobayashi
University of Washington
Department of Mechanical Engineering
Seattle, Washington 98105

Professor Daniel Frederick
Virginia Polytechnic Institute and
State University
Department of Engineering Mechanics
Blacksburg, Virginia 24061

Professor A. C. Eringen
Princeton University
Department of Aerospace and
Mechanical Sciences
Princeton, New Jersey 08540

Professor E. H. Lee
Stanford University
Division of Engineering Mechanics
Stanford, California 94305

Professor Albert I. King
Wayne State University
Biomechanics Research Center
Detroit, Michigan 48202

Dr. V. R. Hodgson
Wayne State University
School of Medicine
Detroit, Michigan 48202

Dean B. A. Boley
Northwestern University
Department of Civil Engineering
Evanston, Illinois 60201

Universities (Con't)

Professor P. G. Hodge, Jr.
University of Minnesota
Department of Aerospace Engineering
and Mechanics
Minneapolis, Minnesota 55455

Dr. D. C. Drucker
University of Illinois
Dean of Engineering
Urbana, Illinois 61801

Professor N. M. Newmark
University of Illinois
Department of Civil Engineering
Urbana, Illinois 61803

Professor E. Reissner
University of California, San Diego
Department of Applied Mechanics
La Jolla, California 92037

Professor William A. Nash
University of Massachusetts
Department of Mechanics and
Aerospace Engineering
Amherst, Massachusetts 01002

Professor G. Herrmann
Stanford University
Department of Applied Mechanics
Stanford, California 94305

Professor J. D. Achenbach
Northwest University
Department of Civil Engineering
Evanston, Illinois 60201

Professor S. B. Dong
University of California
Department of Mechanics
Los Angeles, California 90024

Professor Burt Paul
University of Pennsylvania
Towne School of Civil and
Mechanical Engineering
Philadelphia, Pennsylvania 19104

Universities (Con't)

Professor H. W. Liu
Syracuse University
Department of Chemical Engineering
and Metallurgy
Syracuse, New York 13210

Professor S. Bodner
Technion R&D Foundation
Haifa, Israel

Professor Werner Goldsmith
University of California
Department of Mechanical Engineering
Berkeley, California 94720

Professor R. S. Rivlin
Lehigh University
Center for the Application
of Mathematics
Bethlehem, Pennsylvania 18015

Professor F. A. Cozzarelli
State University of New York at
Buffalo
Division of Interdisciplinary Studies
Karr Parker Engineering Building
Chemistry Road
Buffalo, New York 14214

Professor Joseph L. Rose
Drexel University
Department of Mechanical Engineering
and Mechanics
Philadelphia, Pennsylvania 19104

Professor B. K. Donaldson
University of Maryland
Aerospace Engineering Department
College Park, Maryland 20742

Professor Joseph A. Clark
Catholic University of America
Department of Mechanical Engineering
Washington, D.C. 20064

Universities (Con't)

Dr. Samuel B. Batdorf
University of California
School of Engineering
and Applied Science
Los Angeles, California 90024

Professor Isaac Fried
Boston University
Department of Mathematics
Boston, Massachusetts 02215

Professor E. Krempl
Rensselaer Polytechnic Institute
Division of Engineering
Engineering Mechanics
Troy, New York 12181

Dr. Jack R. Vinson
University of Delaware
Department of Mechanical and Aerospace
Engineering and the Center for
Composite Materials
Newark, Delaware 19711

Dr. J. Duffy
Brown University
Division of Engineering
Providence, Rhode Island 02912

Dr. J. L. Swedlow
Carnegie-Mellon University
Department of Mechanical Engineering
Pittsburgh, Pennsylvania 15213

Dr. V. K. Varadan
Ohio State University Research Foundation
Department of Engineering Mechanics
Columbus, Ohio 43210

Dr. Z. Hashin
University of Pennsylvania
Department of Metallurgy and
Materials Science
College of Engineering and
Applied Science
Philadelphia, Pennsylvania 19104

Universities (Con't)

Dr. Jackson C. S. Yang
University of Maryland
Department of Mechanical Engineering
College Park, Maryland 20742

Professor T. Y. Chang
University of Akron
Department of Civil Engineering
Akron, Ohio 44325

Professor Charles W. Bert
University of Oklahoma
School of Aerospace, Mechanical,
and Nuclear Engineering
Norman, Oklahoma 73019

Professor Satya N. Atluri
Georgia Institute of Technology
School of Engineering and
Mechanics
Atlanta, Georgia 30332

Professor Graham F. Carey
University of Texas at Austin
Department of Aerospace Engineering
and Engineering Mechanics
Austin, Texas 78712

Dr. S. S. Wang
University of Illinois
Department of Theoretical and
Applied Mechanics
Urbana, Illinois 61801

Industry and Research Institutes

Dr. Norman Hobbs
Kaman AviDyne
Division of Kaman
Sciences Corporation
Burlington, Massachusetts 01803

Argonne National Laboratory
Library Services Department
9700 South Cass Avenue
Argonne, Illinois 60440

Industry and Research Institutes (Con't)

Dr. M. C. Junger
Cambridge Acoustical Associates
54 Rindge Avenue Extension
Cambridge, Massachusetts 02140

Dr. V. Godino
General Dynamics Corporation
Electric Boat Division
Groton, Connecticut 06340

Dr. J. E. Greenspon
J. G. Engineering Research Associates
3831 Menlo Drive
Baltimore, Maryland 21215

Newport News Shipbuilding and
Dry Dock Company
Library
Newport News, Virginia 23607

Dr. W. F. Bozich
McDonnell Douglas Corporation
5301 Bolsa Avenue
Huntington Beach, California 92647

Dr. H. N. Abramson
Southwest Research Institute
8500 Culebra Road
San Antonio, Texas 78284

Dr. R. C. DeHart
Southwest Research Institute
8500 Culebra Road
San Antonio, Texas 78284

Dr. M. L. Baron
Weidlinger Associates
110 East 59th Street
New York, New York 10022

Dr. T. L. Geers
Lockheed Missiles and Space Company
3251 Hanover Street
Palo Alto, California 94304

Mr. William Caywood
Applied Physics Laboratory
Johns Hopkins Road
Laurel, Maryland 20810

Industry and Research Institutes (Con't)

Dr. Robert E. Dunham
Pacifica Technology
P.O. Box 148
Del Mar, California 92014

Dr. M. F. Kanninen
Battelle Columbus Laboratories
505 King Avenue
Columbus, Ohio 43201

Dr. A. A. Hochrein
Daedalean Associates, Inc.
Springlake Research Road
15110 Frederick Road
Woodbine, Maryland 21797

Dr. James W. Jones
Swanson Service Corporation
P.O. Box 5415
Huntington Beach, California 92646

Dr. Robert E. Nickell
Applied Science and Technology
3344 North Torrey Pines Court
Suite 220
La Jolla, California 92037

Dr. Kevin Thomas
Westinghouse Electric Corp.
Advanced Reactors Division
P. O. Box 158
Madison, Pennsylvania 15663

UNCLASSIFIED

SECURITY CLASSIFICATION OF THIS PAGE (When Data Entered)

REPORT DOCUMENTATION PAGE

READ INSTRUCTIONS BEFORE COMPLETING FORM

1. REPORT NUMBER: TR No. 39	2. GOVT ACCESSION NO.: A088 287	3. RECIPIENT'S CATALOG NUMBER: TR-39
4. TITLE (and Subtitle): DYNAMIC MIXED MODE FRACTURE		5. TYPE OF REPORT & PERIOD COVERED: Interim Report
		6. PERFORMING ORG. REPORT NUMBER: 39
7. AUTHOR(s): A. S. Kobayashi and M. Ramulu		8. CONTRACT OR GRANT NUMBER(s): N00014-76-C-0060; NR 064-478
9. PERFORMING ORGANIZATION NAME AND ADDRESS: University of Washington, Department of Mechanical Engineering, Seattle, Washington 98195		10. PROGRAM ELEMENT, PROJECT, TASK AREA & WORK UNIT NUMBERS
11. CONTROLLING OFFICE NAME AND ADDRESS: Office of Naval Research, Arlington, Virginia		12. REPORT DATE: August 1980
		13. NUMBER OF PAGES: 10
14. MONITORING AGENCY NAME & ADDRESS (if different from Controlling Office)		15. SECURITY CLASS. (of this report): Unclassified
		15a. DECLASSIFICATION/DOWNGRADING SCHEDULE

16. DISTRIBUTION STATEMENT (of this Report)

Unlimited

This document has been approved for public release and sale; its distribution is unlimited.

17. DISTRIBUTION STATEMENT (of the abstract entered in Block 20, if different from Report)

18. SUPPLEMENTARY NOTES

19. KEY WORDS (Continue on reverse side if necessary and identify by block number)

Fracture Mechanics
Crack Propagation
Crack Arrest
Crack Branching
Fracture Dynamics
Dynamic Photoelasticity
Dynamic Finite Element Analysis

20. ABSTRACT (Continue on reverse side if necessary and identify by block number)

A newly developed data reduction process was used to reevaluate dynamic photoelastic results and to extract dynamic stress intensity factors, K_I^{dyn} and K_{II}^{dyn}, associated with curved and branched cracks in fracturing Homalite-100 plates. A branching stress intensity factor approximately 5 times the fracture toughness was identified for this material. Moderate to severe crack curvings were associated with a K_I^{dyn} and K_{II}^{dyn} ratio as low as 0.05, but with positive remoste stress component, σ_{ox}

DD FORM 1 JAN 73 1473 EDITION OF 1 NOV 65 IS OBSOLETE

S/N 0102-014-6601

UNCLASSIFIED

SECURITY CLASSIFICATION OF THIS PAGE (When Data Entered)